


## Dicke phase transition in a disordered emitter–graphene-plasmon system

Yu-Xiang Zhang,<sup>\*</sup> Yuan Zhang,<sup>†</sup> and Klaus Mølmer<sup>‡</sup>

*Department of Physics and Astronomy, Aarhus University, 8000 Aarhus C, Denmark*

 (Received 9 April 2018; published 19 September 2018)

We study the Dicke phase transition in a disordered system of emitters coupled to the plasmonic modes of a graphene monolayer. This system has unique properties associated with the tunable, dissipative, and broadband characters of the graphene surface plasmons, as well as the disorder due to the random spatial distribution and the inhomogeneous linewidth broadening of the emitters. We apply the Keldysh functional-integral approach and identify a normal phase, a superradiant phase, and a spin-glass phase of the system. The conditions for these phases and their experimental signatures are discussed.

DOI: [10.1103/PhysRevA.98.033821](https://doi.org/10.1103/PhysRevA.98.033821)

### I. INTRODUCTION

The Dicke model [1], which describes the collective coupling between an ensemble of emitters and a radiation field, implies a superradiant (SR) phase [2,3] characterized by a nonzero-electromagnetic-field excitation and a collective atomic polarization [4]. While the validity of the theory predicting the SR phase, especially the proper treatment of  $A^2$  [5] and  $P^2$  terms [6], is still a matter of debate [7–13], the SR phase has now been observed experimentally in cold-atom systems [14–19] where an effective Dicke model is constructed via cavity-assisted Raman transitions [20]. The Dicke model and its phase transitions have also been extended to scenarios with multimode [21–25] and lossy [25–27] cavities, time-dependent couplings [28], and other systems such as superconducting circuits [29,30] and Dicke lattice models [31]. These proposals display the richness of phenomena associated with the collective and superradiant light-matter interaction and stimulate studies of the relation between critical behavior and quantum entanglement [32], quantum chaos [33], and nonequilibrium dynamics [24] in a variety of different physical systems.

In this article we investigate the possibility of observing the Dicke SR phase transition within a system of emitters coupled to surface plasmons (SPs). The SPs are evanescent electromagnetic modes confined near conductor-dielectric interfaces. Their compressed mode volumes enable strong near-field light-emitter couplings [34,35], which make quantum plasmonics a promising platform for quantum optical effects [36,37]. The prediction of superradiance mediated by SPs [38,39] and the recent developments of two-dimensional plasmonic materials [40] and particularly graphene [41], which can be tuned by means of a gate potential [41–43], motivate us to study the Dicke phase transition in systems with graphene SPs (cf. Fig. 1).

The extension of the Dicke model to quantum plasmonics must take into account the broadband SP spectral density

[44–46] and the intrinsic Ohmic losses in the graphene. Thus, the quantization of SPs is more technical than that of optical cavity modes [47–51]. Moreover, the fact that the graphene SP wavelengths are shorter than those of free photons by two orders of magnitudes [42] and could be much shorter than the spatial extent of the emitter ensemble makes it impossible to associate them with a uniform emitter–field coupling strength as commonly used in the Dicke model. Finally, emitters such as rare-earth ions doped in crystals have randomly distributed positions and inhomogeneously broadened transition frequencies. The intrinsic dissipation and disorder will seriously affect the collective coupling to the SP modes, and hence the conditions for the SR phase transition, and allow the presence of a quantum spin-glass phase [52].

This article is organized as follows. In Sec. II we introduce our theoretical approach based on Keldysh functional-integral formalism. The phase diagrams are shown and discussed in Sec. III. Further discussion and an outlook are presented in Sec. IV.

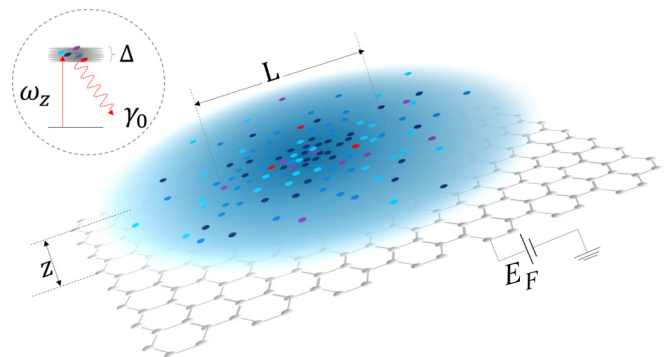


FIG. 1. Emitter-graphene system. An ensemble of  $N$  emitters with spontaneous-emission rate  $\gamma_0$  and transition frequency inhomogeneously broadened by  $\Delta$  around a central transition frequency  $\omega_z$  is distributed in a layer with horizontal dimension  $L$  at height  $z$ . The Fermi energy  $E_F$  of the graphene electrons can be tuned by gate doping.

<sup>\*</sup>iyxz@phys.au.dk

<sup>†</sup>yzhang@phys.au.dk

<sup>‡</sup>moelmer@phys.au.dk

## II. THEORY AND METHODS

To describe the disordered emitter-graphene system illustrated in Fig. 1, we will establish a Keldysh functional-integral approach, which takes the field losses due to the coupling with medium into account [47].

### A. Quantization of the dispersive and dissipative light field

A bosonic field  $\mathbf{f}(\mathbf{r}, \tilde{\omega})$ , with three Cartesian components  $f_a$ , position  $\mathbf{r}$ , and frequency  $\tilde{\omega}$ , can be defined with the commutators  $[f_a(\mathbf{r}_1, \tilde{\omega}_1), f_b^\dagger(\mathbf{r}_2, \tilde{\omega}_2)] = \delta_{ab}\delta(\mathbf{r}_1 - \mathbf{r}_2)\delta(\tilde{\omega}_1 - \tilde{\omega}_2)$ ,  $[f_a, f_b] = 0$ , and  $[f_a^\dagger, f_b^\dagger] = 0$  such that the quantized electric field can be written as [49–51]

$$\mathbf{E}(\mathbf{r}) = i\mu_0\sqrt{\frac{\hbar\epsilon_0}{\pi}} \int_0^\infty d\tilde{\omega} \int d^3\mathbf{r}' \tilde{\omega}^2 \sqrt{\text{Im } \epsilon(\mathbf{r}', \tilde{\omega})} \times \mathbf{G}(\mathbf{r}, \mathbf{r}', \tilde{\omega}) \cdot \mathbf{f}(\mathbf{r}', \tilde{\omega}) + \text{H.c.}, \quad (1)$$

where  $\mathbf{G}(\mathbf{r}, \mathbf{r}', \tilde{\omega})$  is the dyadic Green's tensor,  $\mu_0$  and  $\epsilon_0$  are the vacuum susceptibility and permittivity, respectively,  $\text{Im } \epsilon$  stands for the imaginary part of the relative permittivity, and H.c. is short for Hermitian conjugate. Equation (1) resembles the particular solution to Maxwell's equations associated with a quantized current source  $\tilde{\omega}\sqrt{\hbar\epsilon_0}\text{Im } \epsilon(\mathbf{r}', \tilde{\omega})/\pi\mathbf{f}(\mathbf{r}', \tilde{\omega})$ .

The Hamiltonian of the system studied by us can be written as

$$H = H_0 + \sum_{i=1}^N \left[ \frac{1}{2}\hbar\omega_{i,z}\sigma_i^z - \sigma_i^x \mathbf{d}_i \cdot \mathbf{E}(\mathbf{r}_i) \right], \quad (2)$$

where  $H_0 = \int d^3\mathbf{r}' \int_0^\infty d\tilde{\omega} \hbar\tilde{\omega}\mathbf{f}^\dagger(\mathbf{r}', \tilde{\omega})\mathbf{f}(\mathbf{r}', \tilde{\omega})$  is the free-field Hamiltonian and  $\omega_{i,z}$ ,  $\mathbf{d}_i$ , and  $\mathbf{r}_i$  are the transition frequency, dipole, and position of the  $i$ th emitter, respectively. We model the emitters as two-level systems with Pauli operators  $\sigma_i^z$  and  $\sigma_i^x$ . Notice that here the rotating-wave approximation is not used.

The Hamiltonian in the form of Eq. (2) has been widely used in the literature and should be interpreted within the multipolar gauge and the term  $\mathbf{E}(\mathbf{r}_i)$  of Eq. (2) should be understood as  $\frac{1}{\epsilon(\mathbf{r}_i)\epsilon_0}\mathbf{D}(\mathbf{r}_i)$ , where  $\mathbf{D}(\mathbf{r}_i)$  is the displacement field [8–11]. Equation (2) further assumes that the distance between any two emitters is larger than the size of the atoms, since otherwise a residual instantaneous interatomic potential must be included in the treatment [10,11]. Notice that the experimental observations of the SR phase transitions are based on effective Dicke models employing Raman processes [14–20]. Our theory can be generalized straightforwardly to the quantum plasmonic version of these models [53].

### B. Keldysh functional-integral approach

The Keldysh functional-integral approach is convenient for the analysis of open-system nonequilibrium dynamics

in disordered systems [24]. To apply it, the Pauli operators representing the two-level emitters are replaced by a real bosonic variable  $\phi_i(t)$  with unit length, i.e.,  $\phi_i^2(t) = 1$  [24],

$$\sigma_i^x(t) \rightarrow \phi_i(t), \quad \sigma_i^z(t) \rightarrow \frac{2}{\omega_{i,z}^2}(\partial_t\phi_i)^2 - 1. \quad (3)$$

This mapping originates from the correspondence between the energy gap of quantum models and the correlation length along the time direction of their classical counterparts and works well for phase transitions [23–26] (see Refs. [54–57] for further details). The Keldysh action of the free emitters derived from Eq. (2) is then expressed as (see Appendix A)

$$S_e = - \sum_{i=1}^N \int_{C_a} dt \left[ \frac{1}{\omega_{i,z}}(\partial_t\phi_{i,a})^2 + \lambda_{i,a}(t)(\phi_{i,a}^2 - 1) \right], \quad (4)$$

where  $\lambda_{i,a}$  is the Lagrange multiplier introduced for the restriction  $\phi_{i,a}^2 = 1$  and the variables labeled by  $a = \pm$  are defined along the time-integral contours  $C_\pm = \mp\infty \rightarrow \pm\infty$  (for steady states, we do not need to specify initial states [58]).

In the Keldysh functional-integral approach, we can formally integrate out the degrees of freedom of  $\mathbf{f}(\mathbf{r}, \tilde{\omega})$  and get the Keldysh action for the emitter-emitter coupling mediated by them (see Appendix B)

$$S_{ee}^{(p)} = \sum_{i,j=1}^N \int_{-\infty}^{\infty} \frac{d\omega}{2\pi} (\phi_{i,c} \quad \phi_{i,q})_{-\omega} \times \begin{pmatrix} 0 & h_{ij}^*(\omega) \\ h_{ij}(\omega) & 2i \text{Im } h_{ij}(|\omega|) \end{pmatrix} \begin{pmatrix} \phi_{j,c} \\ \phi_{j,q} \end{pmatrix}_{\omega}, \quad (5)$$

where the  $\omega$ -dependent coupling strength is

$$h_{ij}(\omega) = \frac{\omega^2}{2\hbar\epsilon_0c^2} \mathbf{d}_i \cdot \mathbf{G}(\mathbf{r}_i, \mathbf{r}_j, \omega) \cdot \mathbf{d}_j. \quad (6)$$

Note that we have passed to the Fourier domain with frequency variable  $\omega$  and have transformed to the so-called classical (quantum) fields  $\phi_{i,c(q)}$  by the Keldysh rotation  $\phi_{i,c(q)} = [\phi_{i,+} + (-)\phi_{i,-}]/\sqrt{2}$  [24]. The corresponding transformation of the Lagrange multipliers  $\lambda_{i,c(q)}$  is  $\lambda_{i,c(q)} = \lambda_{i,+} + (-)\lambda_{i,-}$ .

### C. Spatial disorders

To treat the disorder in the emitter system, we follow the strategy of random-bond models widely used in the studies of spin glasses [59]. That is, the real and imaginary parts of the coupling strength  $\{\text{Re } h_{ij}(\omega), \text{Im } h_{ij}(\omega)\}_{i \neq j}$ , which are functionals of the emitter positions and dipoles, are viewed as random variables following a multicomponent Gaussian distribution (neglecting higher-order moments) with the mean and the covariance given by

$$\bar{h}_{(2)}(\omega) = \int d^3\mathbf{r}_a d^3\mathbf{r}_b p(\mathbf{r}_a, \mathbf{r}_b) h_{ab}(\omega), \quad (7a)$$

$$M(\omega, \omega') = \int d^3\mathbf{r}_a d^3\mathbf{r}_b p(\mathbf{r}_a, \mathbf{r}_b) \begin{pmatrix} \delta \text{Re } h_{ab}(\omega) \delta \text{Re } h_{ab}(\omega') & \delta \text{Re } h_{ab}(\omega) \delta \text{Im } h_{ab}(\omega') \\ \delta \text{Im } h_{ab}(\omega) \delta \text{Re } h_{ab}(\omega') & \delta \text{Im } h_{ab}(\omega) \delta \text{Im } h_{ab}(\omega') \end{pmatrix}, \quad (7b)$$

where  $p(\mathbf{r}_a, \mathbf{r}_b)$  denotes the probability distribution of the positions of two emitters (the average over  $\{\mathbf{d}_i\}$  is implicitly assumed) and  $\delta$  denotes the difference with respect to the mean value of the real and imaginary parts of  $\bar{h}_{(2)}(\omega)$ . For the emitter-graphene system to be investigated later, the individual terms  $h_{ii}(\omega)$  are identical for all  $i$ , since they are determined only by the height  $z$  of the emitter layer over the graphene. We will denote their values by  $\bar{h}_{(1)}(\omega)$ .

#### D. Inhomogeneous broadening

Emitters such as rare-earth ions doped in crystals experience inhomogeneous broadening of their transition spectrum (cf. Fig. 1). To take this into account, the conventional method is to divide the ensemble into groups of emitters with the same transition frequency [31,60]. Here we do not follow this method but rather assume the transition frequency  $\omega_{i,z}$  follows a Gaussian distribution centered at  $\omega_z$  with standard deviation  $\Delta$ . Thus, the broadening can be treated statistically and contributes a new term to the Keldysh action of the system

$$S^{(b)} = i \frac{\Delta^2}{2\omega_z^4} \sum_{i=1}^N \left( \int d\omega \omega^2 \phi_{i,c}(-\omega) \phi_{i,q}(\omega) \right)^2. \quad (8)$$

In Appendix E we show that the main effect of  $S^{(b)}$  is to shift the covariance  $M(\omega, \omega')$  defined in Eq. (7b) by terms that scale as  $(\Delta \frac{\omega\omega'}{\omega_z^2})^2$  and are negligible for a large  $N$ .

#### E. Order parameters

To distinguish the different phases of the system, we introduce the order parameters [24–26,56,57,59]

$$\begin{aligned} Q_{\alpha\beta}(\omega, \omega') &= -i \frac{1}{N} \sum_{i=1}^N \langle \phi_{i,\alpha}(\omega) \phi_{i,\beta}(\omega') \rangle, \\ \psi_\alpha(\omega) &= -\frac{1}{N} \sum_{i=1}^N \langle \phi_{i,\alpha}(\omega) \rangle, \end{aligned} \quad (9)$$

where  $\alpha, \beta \in \{c, q\}$ . In addition,  $Q_{cq}$ ,  $Q_{qc}$ , and  $Q_{cc}$  are the retarded, advanced, and Keldysh Green's functions of the emitters [24], respectively. Further,  $\psi_c$  is the average polarization of the emitters. For the steady state, we substitute the ansatz that  $\psi_\alpha(\omega) = 2\pi\delta(\omega)\psi_\alpha$ ,  $\lambda_{i,\alpha}(\omega) = 2\pi\delta(\omega)\lambda_{i,\alpha}$ , and  $Q_{\alpha\beta}(\omega, \omega') = 2\pi\delta(\omega + \omega')Q_{\alpha\beta}(\omega)$  and introduce the Edward-Anderson order parameter  $q_{EA}$  [23–25,52,55,59] to pin down the spin-glass phase

$$Q_{cc}(\omega) = Q_{cc}^{\text{reg}}(\omega) - i2\pi q_{EA}\delta(\omega), \quad (10)$$

where reg labels the regular part. In the time domain, we have  $q_{EA} \propto \lim_{t \rightarrow \infty} \frac{1}{N} \sum_i \langle \sigma_i^x(t) \sigma_i^x(0) \rangle$ . Thus a finite  $q_{EA}$  implies an infinite correlation time of the individual emitter dipoles.

The steady state of the system and the values of the order parameters are determined by the saddle-point equations of the Keldysh action (see Appendix D). This leads to the identification of three different phases: the SR phase with  $q_{EA} \neq 0$  and  $\psi_c \neq 0$ , the spin-glass (SG) phase [59] with  $q_{EA} \neq 0$  and  $\psi_c = 0$ , and the normal phase with  $q_{EA} = 0$  and  $\psi_c = 0$  where no symmetry of the Hamiltonian is broken. The criterion in terms of the system parameters for the SR-SG

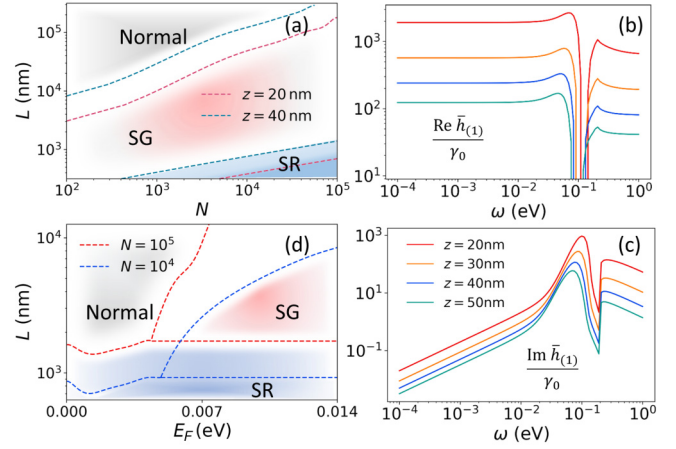


FIG. 2. Results for systems with  $\omega_z = 0.5$  eV and  $E_F = 0.1$  eV: (a) the  $N$ - $L$  phase diagram for  $\gamma_0 = 10^{-5}$  eV, with different normal-SG and SG-SR boundaries for  $z = 20$  nm (red lower dashed curves) and  $z = 40$  nm (upper dashed curves); (b) the value of  $\text{Re} \bar{h}_{(1)}(\omega)$ , the energy shift induced by graphene; (c) the value of  $\text{Im} \bar{h}_{(1)}(\omega)$ , the graphene-induced emitter damping, as a function of frequency and different heights for  $z = 20$  nm (red top curve),  $z = 30$  nm (orange curve),  $z = 40$  nm (blue curve),  $z = 50$  nm (green bottom curve); and (d) the  $E_F$ - $L$  phase diagram for  $z = 50$  nm,  $\gamma_0 = 10^{-8}$  eV, and different normal-SG and SG-SR boundaries for  $N = 10^4$  (blue lower dashed curves) and  $N = 10^5$  (red upper dashed curves).

transition has an analytical solution while the other phase boundaries are governed by integral equations that have to be solved numerically.

### III. RESULTS

We model the system depicted in Fig. 1 as a layer of  $N$  emitters positioned at a distance  $z$  over the graphene monolayer. The emitter dipoles  $\{\mathbf{d}_i\}_i$  are aligned to be perpendicular to the graphene layer and their magnitudes are quantified by the spontaneous-emission rate  $\gamma_0$ . The graphene is modeled as a two-dimensional surface with conductivity  $\sigma(E_F, \tau; \omega)$  [61] given in the local random-phase approximation [42], where  $E_F$  is the Fermi energy tunable by gate doping and  $\tau$  is the relaxation time accounting for the electron-phonon scattering (we use  $\tau = 1$  ps as a characteristic value between 0.1 ns predicted by theory [62] and 500 fs observed in experiments [63]). The in-plane positions of the emitters are assumed to follow independent Gaussian distributions with width  $L$ . Our results thus depend on the set of parameters  $N$ ,  $L$ ,  $z$ ,  $E_F$ ,  $\omega_z$ ,  $\gamma_0$ , and  $\Delta$ . To focus on the phase transitions associated with the graphene SP, we will truncate the environment modes by replacing the total dyadic Green's function by its scattering part, which contains the information of the graphene SP (see Appendix F for more details). Other channels of emitter decay and dephasing are not considered because their effects are negligible when their rates are small compared with  $\omega_z$  [27].

Figure 2(a) shows the location of the phase transitions as a function of the ensemble size and number of emitters. It demonstrates that the SR phase favors higher emitter densities. We also find that the phase diagram changes only little due to inhomogeneous broadening: For  $z = 20$  nm and  $N =$

100 the normal-SG phase boundary shifts  $L$  downward by only about 60 nm for a broadening as large as  $\Delta = 0.1$  eV (here and throughout,  $\hbar = 1$ ).

Although smaller  $z$  implies stronger emitter-graphene SP couplings, Fig. 2(a) shows that when the emitters are moved from the  $z = 40$  nm to  $z = 20$  nm distance to the graphene, the normal-SG and SG-SR phase boundaries shift downward, i.e., they occur for higher emitter densities. When  $z$  is decreased, there is a complicated interplay between the enhanced SP-induced energy shift [see Fig. 2(b)], leading to the Dicke SR phase, and the increased damping of the emitters, due to the same coupling [see Fig. 2(c)]. The competition between these effects is the main cause for the shift of the phase-transition boundaries. We note, however, that for extremely small  $z$ , emitter-graphene bound states may form [64–68], so different behavior, including polarization of the emitters, should be expected.

One may try to understand the SR phase of our system by comparing it with the Dicke model of a single-cavity mode, where the effective emitter-emitter coupling Hamiltonian is given by  $H_{\text{eff}} = -\sum_{i,j} J \sigma_i^x \cdot \sigma_j^x$ ,  $J = g^2 \omega_c / (\omega_c^2 - \omega^2)$  [23], and the SR phase is reached when  $g^2 N > \omega_z \omega_c / 4$ . In our model,  $\text{Re } h_{ij}(\omega)$  plays the role of  $J$  and the mean  $\text{Re } \bar{h}_{(2)}(\omega)$  does not meet the equivalent SR criterion. However, smaller-size subensembles of emitters might experience strong enough mutual coupling. This fact is indicated by the large fluctuations of  $\text{Re } h_{ij}(\omega)$  resulting from the disorders, which are shown in Figs. 4(e) and 4(f) of Appendix F. Such subensembles would contribute significantly to the averaged polarization  $\psi_c$  of the system of emitters and lead to the SR phase. To properly account for the role of such subensembles, a more refined description than the current mean-field approach will be required. A similar relaxation of the SR criterion on the average coupling strength occurs for the Dicke models with parameter fluctuations [23,69].

In the following we discuss the effect of tuning the Fermi energy  $E_F$ , a possibility unique to graphene. The SG-SR phase boundary is insensitive to  $E_F$  (see Appendix F). A higher  $E_F$ , however, leads to stronger graphene SP-induced emitter-emitter coupling [42,43] and facilitates the normal-SG phase transition as shown in the phase diagram of Fig. 2(d). It also shows a triple point and the normal-SR phase boundary which are absent in Fig. 2(a). However, there is also a subtle SR to normal to SR transition with an increasing  $E_F$ .

To understand it, we borrow ideas from the studies of spin-boson models [44–46], which suggest that the following three quantities might be pertinent: the emitter spectral response yield from the emitter linear susceptibility  $A^{\text{SR}}(\omega) = -2 \text{Im } Q_{cq}$ , the spectral density  $\text{Im } \bar{h}_{(1)}(\omega)$ , and the many-spin extension of the spectral density  $\text{Im } \bar{h}_{(2)}(\omega)$ . The spectral density is the central concept of models where a single spin couples to a continuum of bosons [44]. We note that only  $A^{\text{SR}}(\omega)$  depends on  $\omega_z$  [23], while  $\text{Im } \bar{h}_{(1)}(\omega)$  and  $\text{Im } \bar{h}_{(2)}(\omega)$  depend on the magnitude of the emitter dipoles quantified by  $\gamma_0/\omega_z^3$ .

To look closer at the normal-SR transition, we depict an  $E_F$ - $\omega_z$  phase diagram in Fig. 3 for different values of  $\gamma_0/\omega_z^3$ . The frequency dependence of  $A^{\text{SR}}$ ,  $\text{Im } \bar{h}_{(1)}$ , and  $\text{Im } \bar{h}_{(2)}$  is shown in Fig. 3 for the four different Fermi energies

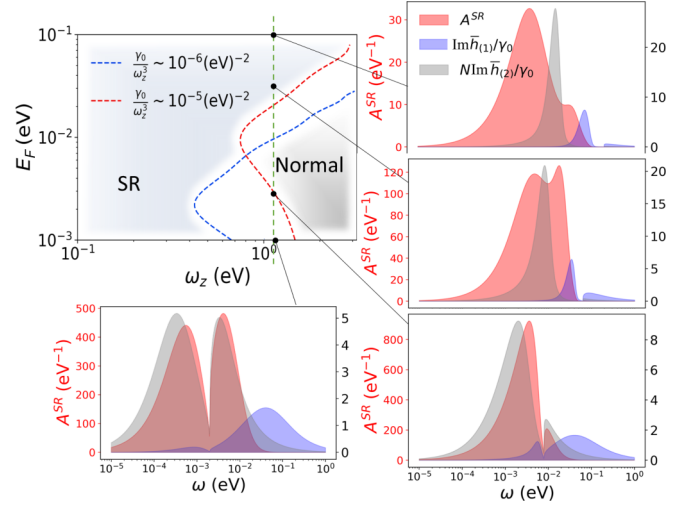


FIG. 3. The  $E_F$ - $\omega_z$  phase diagram for a system with  $z = 50$  nm,  $L = 10^3$  nm,  $N = 2 \times 10^4$ , and two different values of  $\gamma_0/\omega_z^3$  so that when  $\omega_z = 0.5$  eV,  $\gamma_0 = 10^{-7}$  (blue lower dashed curve) or  $10^{-6}$  eV (red upper dashed curve). For the case of  $\omega_z = 1$  eV, the spectral densities  $A^{\text{SR}} = -2 \text{Im } Q_{cq}(\omega)$  (red shaded, darkest),  $\text{Im } \bar{h}_{(1)}$  (blue shaded, peaks at the right-hand side), and  $\text{Im } \bar{h}_{(2)}$  (gray shaded, lightest) are shown for different Fermi energies  $E_F = 0.1, 0.032, 0.004, 0.001$  eV. The values of  $\text{Im } \bar{h}_{(1,2)}$  are shown on the right-hand vertical axes.

$E_F = 0.1, 0.032, 0.004, 0.001$  eV. There are gaps between the positions of the peaks of  $\text{Im } \bar{h}_{(1)}(\omega)$  and those of  $\text{Im } \bar{h}_{(2)}(\omega)$  because the short-range modes, important for the self-interaction term  $\text{Im } \bar{h}_{(1)}(\omega)$ , cannot propagate far enough to affect the averaged emitter-emitter coupling. Changing  $E_F$  shifts the peaks of  $A^{\text{SR}}$ ,  $\text{Im } \bar{h}_{(1)}$ , and  $\text{Im } \bar{h}_{(2)}$  and we observe a closer overlap of  $A^{\text{SR}}(\omega)$  with  $\text{Im } \bar{h}_{(1)}(\omega)$ , reflecting the influence of the SP-induced emitter decay, when the system is closer to the regime of the normal phase. For the number of emitters  $N$  applied here,  $\text{Im } \bar{h}_{(1)}(\omega)$  and  $N \text{Im } \bar{h}_{(2)}(\omega)$  are comparable and suggest that the subtle  $E_F$  dependence of the phase transition observed in Figs. 2(d) and 3 is a finite- $N$  effect relevant to the graphene SP-induced emitter decay.

Additionally, the peaks of  $A^{\text{SR}}$  and  $\text{Im } \bar{h}_{(1,2)}$  shown in Fig. 3 generally occur far from the emitter resonance  $\omega_z$ . This indicates that the influence of the inhomogeneous broadening, which scales as  $(\Delta \frac{\omega \omega'}{\omega_z})^2$ , is small. Moreover, their marked frequency dependence invalidates the Markov approximation, which would replace  $\text{Im } \bar{h}_{1,2}(\omega)$  by a constant taken at the emitter transition energy [67,68,70,71]. Indeed, our formalism considers the full spectral dependences and does not apply the Markov approximation.

#### IV. SUMMARY AND OUTLOOK

To summarize, applying the Keldysh functional-integral approach, we have studied the Dicke phase transitions between the superradiance phase, the spin-glass phase, and the normal phase in a disordered emitter-graphene-surface-plasmon system. Our formalism is a generalization of the spin-boson model [44] to the many-spin system and is valid for general plasmonic systems. The variety of nanoscale plas-

monic systems, and especially two-dimensional materials like the graphene monolayer, constitute excellent platforms to test the fundamental collective phenomena of the Dicke model and its effects in quantum optics, nonequilibrium dynamics of driven dissipative system, and condensed matter physics. The presence of the spin-glass phase indicates interesting relations with the Hopfield neural network and associative memory [72,73].

The superradiant phase is characterized by the emitter polarization. The spin-glass phase behaves differently from the superradiant phase at the low-frequency regime of the emitter spectral response  $-2\text{Im} Q_{cq}(\omega)$  [24–26]. Thus they may be distinguished by observing their radio-frequency spectral response [74,75]. By employing an optical cavity, it may be possible to observe a hybrid coupling of the emitters to both surface plasmons and a cavity mode and to use the cavity response and transmission spectrum as a signature of the surface plasmon Dicke phase transition [20,25].

As in most treatments of the superradiant phase transition (for exceptions, see, e.g., Refs. [7,13,76]), the effect of the Coulomb dipole-dipole couplings is omitted due to inclusion of only the scattering part of the total dyadic Green's function. To properly include the variations in the dipole-dipole coupling strengths within the emitter ensemble [77] and short-range instantaneous interaction relevant at high densities [10,11], it is necessary to go beyond the Gaussian distribution assumed in this article.

### ACKNOWLEDGMENTS

We sincerely thank Frank Koppens, Klass-Jan Tielrooij, Daniel Cano Reol, and Darrick Chang for useful discussions and suggestions. This work was supported by European Unions Horizon 2020 research and innovation program (Grant No. 712721, NanoQtech) and the Villum Foundation.

### APPENDIX A: ACTION OF THE FREE EMITTERS

The Keldysh action of a system with Hamiltonian  $H$  is formulated by representing the dynamical variables by  $\psi$  according to [24]

$$S = \int dt [\psi_+^* i \partial_t \psi_+ - \psi_-^* i \partial_t \psi_- - (H_+ - H_-)]. \quad (\text{A1})$$

We employ two sets of bosonic variables,  $\phi_i$  for the emitters and  $\mathbf{f}(\mathbf{r}', \tilde{\omega})$  for the electromagnetic environment.

The Keldysh action for the free emitters is given as Eq. (4) and is derived from Eq. (A1) with the mapping

$$\sigma_i^x(t) \rightarrow \phi_i(t), \quad \sigma_i^z(t) \rightarrow \frac{2}{\omega_c^2} (\partial_t \phi_i)^2 - 1, \quad (\text{A2})$$

where we have omitted the effect of inhomogeneous broadening. Discussion on that is deferred to Appendix E. Then we substitute  $\phi_i(t)$  into Eq. (A1). Since  $\phi_i(t)$  is a real variable, the first two terms of Eq. (A1) are time-derivative terms, that is,  $\phi_i^* i \partial_t \phi_i = \phi_i i \partial_t \phi_i = \frac{1}{2} i \partial_t (\phi_i^2)$ . These terms are negligible because they have no effect on the action after the integral over time.

The restriction  $\phi^2(t) = 1$  is imposed by multiplying the Keldysh partition function by the  $\delta$  functions  $\prod_t \delta(\phi_{\pm}^2(t) -$

1). This process brings Lagrange multipliers  $\lambda_{\pm}(t)$  to the action according to the relation that

$$\prod_t \delta(\phi_{\pm}^2(t) - 1) = \int D\lambda_{\pm}(t) \exp \left( i \int dt \lambda_{\pm}(t) [\phi_{\pm}^2(t) - 1] \right). \quad (\text{A3})$$

Then we perform the Keldysh rotation, a unitary transformation of the contour index

$$\begin{aligned} \phi_c &= \frac{1}{\sqrt{2}}(\phi_+ + \phi_-), & \phi_q &= \frac{1}{\sqrt{2}}(\phi_+ - \phi_-), \\ \lambda_c &= \lambda_+ + \lambda_-, & \lambda_q &= \lambda_+ - \lambda_-, \end{aligned} \quad (\text{A4})$$

where the subscripts  $c$  and  $q$  stand for classical and quantum, respectively [24]. The constraint equation then amounts to inclusion of the Lagrange multiplier term

$$2 \int_t \lambda_c(t) \phi_c(t) \phi_q(t) + \lambda_q(t) [\phi_c^2(t) + \phi_q^2(t) - 2] \quad (\text{A5})$$

in the action, where  $\int_t$  is shorthand for  $\int dt$ . Retaining only its static contribution, we use the ansatz that

$$\lambda_{i,\alpha}(\omega) = 2\pi \lambda_{i,\alpha} \delta(\omega) \quad (\text{A6})$$

in the Fourier domain, where  $\alpha \in \{c, q\}$ . Finally, the Keldysh action of the free emitters is written as

$$\begin{aligned} S_e &= \sum_{i=1}^N \int_w (\phi_{i,c}, \phi_{i,q})_{-\omega} \begin{pmatrix} \lambda_{i,q} & \lambda_{i,c} - \frac{\omega^2}{\omega_c^2} \\ \lambda_{i,c} - \frac{\omega^2}{\omega_c^2} & \lambda_{i,q} \end{pmatrix} \\ &\times \begin{pmatrix} \phi_{i,c} \\ \phi_{i,q} \end{pmatrix}_{\omega} - 2 \sum_{i=1}^N \lambda_{i,q} 2\pi \delta(0), \end{aligned} \quad (\text{A7})$$

where  $\int_w$  is shorthand for  $\int \frac{d\omega}{2\pi}$ .

### APPENDIX B: ACTION FOR THE PLASMONIC ENVIRONMENT

The plasmonic electromagnetic environment is quantized through the complex field  $\mathbf{f}(\mathbf{r}', \tilde{\omega})$ . Here we denote it by  $f_{a,\mathbf{r},\tilde{\omega}}$ , where  $a$  labels the three Cartesian directions. The Keldysh action of the free plasmonic environment and its coupling to the emitters is

$$\begin{aligned} S_{f,ef} &= \sum_a \int_{\tilde{\omega}, \mathbf{r}, \omega} (f_{a,\mathbf{r},\tilde{\omega};c}^* \quad f_{a,\mathbf{r},\tilde{\omega};q}^*)_{\omega} D_{\tilde{\omega}}(\omega) \begin{pmatrix} f_{a,\mathbf{r},\tilde{\omega};c} \\ f_{a,\mathbf{r},\tilde{\omega};q} \end{pmatrix}_{\omega} \\ &- \sum_{i=1}^N \sum_a \int_{\tilde{\omega}, \mathbf{r}', \omega} g_{ia}(\mathbf{r}', \tilde{\omega}) \\ &\times [\phi_{i,-\omega;c} f_{a,\mathbf{r}',\tilde{\omega};q}(\omega) + \phi_{i,-\omega;q} f_{a,\mathbf{r}',\tilde{\omega};c}(\omega)] \\ &+ g_{ia}^*(\mathbf{r}', \tilde{\omega}) [\phi_{i,\omega;c} f_{a,\mathbf{r}',\tilde{\omega};q}^*(\omega) + \phi_{i,\omega;q} f_{a,\mathbf{r}',\tilde{\omega};c}^*(\omega)], \end{aligned} \quad (\text{B1})$$

where  $\int_{\tilde{\omega}}$  is shorthand for  $\int_0^{\infty} \frac{d\tilde{\omega}}{2\pi}$ ,  $\int_{\mathbf{r}'}$  is shorthand for  $\int d^3\mathbf{r}'$ , the matrix  $D_{\tilde{\omega}}(\omega)$  is defined as

$$D_{\tilde{\omega}}(\omega) = \begin{pmatrix} 0 & \omega - \tilde{\omega} - i\epsilon \\ \omega - \tilde{\omega} + i\epsilon & 2i\epsilon \end{pmatrix}, \quad (\text{B2})$$

and  $\epsilon$  stands for an infinitesimal positive constant; the coupling strength is

$$g_{ia}(\mathbf{r}', \tilde{\omega}) = -i \sqrt{\frac{\epsilon_I(\mathbf{r}', \tilde{\omega}) \tilde{\omega}^2}{\hbar \pi \epsilon_0 c^2}} \sum_b \mathbf{d}_{ib} \mathbf{G}_{ba}(\mathbf{r}_i, \mathbf{r}', \tilde{\omega}). \quad (\text{B3})$$

In Eq. (B1) all terms with identical indices of  $\tilde{\omega}$  and  $\omega$  share the same matrix  $D_{\tilde{\omega}}(\omega)$ . Therefore, after integrating out the field of  $\mathbf{f}(\mathbf{r}, \tilde{\omega})$ ,  $S_{f,ef}$  turns out to be an effective emitter-emitter coupling action

$$S_{ee}^{(p)} = - \sum_{i,j=1}^N \int_{\tilde{\omega}, \omega} \tilde{g}_{ij}(\tilde{\omega}) (\phi_{i,c} \quad \phi_{i,q})_{-\omega} \sigma_x D_{\tilde{\omega}}^{-1} \sigma_x \begin{pmatrix} \phi_{j,c} \\ \phi_{j,q} \end{pmatrix}_{\omega}, \quad (\text{B4})$$

where the coupling strength  $\tilde{g}_{ij}(\tilde{\omega})$  is

$$\begin{aligned} \tilde{g}_{ij}(\tilde{\omega}) &= \sum_a \int_{\mathbf{r}'} g_{ia}(\mathbf{r}', \tilde{\omega}) g_{ja}^*(\mathbf{r}', \tilde{\omega}) \\ &= \frac{1}{\pi \epsilon_0 \hbar c^2} \tilde{\omega}^2 \mathbf{d}_i \cdot \text{Im} \mathbf{G}(\mathbf{r}_i, \mathbf{r}_j, \tilde{\omega}) \cdot \mathbf{d}_j \end{aligned} \quad (\text{B5})$$

and  $\sigma_x$  is the matrix  $\begin{pmatrix} 0 & 1 \\ 1 & 0 \end{pmatrix}$ . In the derivation of  $\tilde{g}_{ij}$ , we have used the relation

$$\begin{aligned} \sum_b \frac{\omega^2}{c^2} \int_{\mathbf{r}'} \epsilon_I(\mathbf{r}', \omega) \mathbf{G}_{ab}(\mathbf{r}_i, \mathbf{r}', \omega) \mathbf{G}_{cb}^*(\mathbf{r}_j, \mathbf{r}', \omega) \\ = \text{Im} \mathbf{G}_{ac}(\mathbf{r}_i, \mathbf{r}_j, \omega). \end{aligned} \quad (\text{B6})$$

The inverse of  $D_{\tilde{\omega}}(\omega)$  is expressed as

$$D_{\tilde{\omega}}^{-1}(\omega) = \begin{pmatrix} \frac{-2i\epsilon}{(\omega - \tilde{\omega})^2 + \epsilon^2} & \frac{1}{\omega - \tilde{\omega} + i\epsilon} \\ \frac{1}{\omega - \tilde{\omega} - i\epsilon} & 0 \end{pmatrix}. \quad (\text{B7})$$

Then, using the relations

$$\begin{aligned} \lim_{\epsilon \rightarrow 0^+} \frac{\epsilon}{(\omega - \omega_\mu)^2 + \epsilon^2} &= \pi \delta(\omega - \omega_\mu), \\ \lim_{\epsilon \rightarrow 0^+} \frac{1}{\omega - \omega_\mu \pm i\epsilon} &= \mathcal{P} \frac{1}{\omega - \omega_\mu} \mp i\pi \delta(\omega - \omega_\mu), \end{aligned} \quad (\text{B8})$$

we can implement the integral of  $\tilde{\omega}$  in  $S_{ee}^{(p)}$ , i.e.,

$$\Lambda(\omega) = \int_{\tilde{\omega}} \tilde{g}_{ij}(\tilde{\omega}) \sigma_x D_{\tilde{\omega}}^{-1}(\omega) \sigma_x. \quad (\text{B9})$$

The result is

$$\Lambda(\omega) = \begin{pmatrix} 0 & F_{ij}(\omega) + i\pi \Delta_{ij}(\omega) \\ F_{ij}(\omega) - i\pi \Delta_{ij}(\omega) & -2i\pi \Delta_{ij}(\omega) \end{pmatrix}, \quad (\text{B10})$$

where the elements of the matrix are

$$F_{ij}(\omega) = \int_{\tilde{\omega}} \frac{\tilde{\omega}^2}{\pi \epsilon_0 \hbar c^2} \mathbf{d}_i \cdot \text{Im} \mathbf{G}(\mathbf{r}_i, \mathbf{r}_j, \tilde{\omega}) \cdot \mathbf{d}_j \mathcal{P} \frac{1}{\omega - \tilde{\omega}}, \quad (\text{B11a})$$

$$\Delta_{ij}(\omega) = \int_{\tilde{\omega}} \frac{\tilde{\omega}^2}{\pi \epsilon_0 \hbar c^2} \mathbf{d}_i \cdot \text{Im} \mathbf{G}(\mathbf{r}_i, \mathbf{r}_j, \tilde{\omega}) \cdot \mathbf{d}_j \delta(\omega - \tilde{\omega}). \quad (\text{B11b})$$

Due to the symmetry of the indices, we reshape  $\Lambda(\omega)$  by

$$\Lambda(\omega) \rightarrow \frac{1}{2} [\Lambda(\omega) + \Lambda^\top(-\omega)], \quad (\text{B12})$$

where  $\top$  stands for matrix transposition. Then the elements of  $\Lambda(\omega)$  are modified to

$$\begin{aligned} \Lambda_{22} &\rightarrow -i\pi [\Delta_{ij}(\omega) + \Delta_{ij}(-\omega)] \\ &= \frac{-i\omega^2}{\hbar \epsilon_0 c^2} \mathbf{d}_i \cdot \text{Im} \mathbf{G}(\mathbf{r}_i, \mathbf{r}_j, |\omega|) \cdot \mathbf{d}_j \\ &= \text{sgn}(\omega) \frac{-i\omega^2}{\hbar \epsilon_0 c^2} \mathbf{d}_i \cdot \text{Im} \mathbf{G}(\mathbf{r}_i, \mathbf{r}_j, \omega) \cdot \mathbf{d}_j, \end{aligned} \quad (\text{B13})$$

where we have used the relation  $\mathbf{G}(\omega) = \mathbf{G}^*(-\omega)$  and

$$\Lambda_{21} \rightarrow \frac{1}{2} [F_{ij}(\omega) + i\pi \Delta_{ij}(\omega) + F_{ij}(-\omega) - i\pi \Delta_{ij}(-\omega)]. \quad (\text{B14})$$

To evaluate the expressions, we will use the Kramers-Kronig relation. For a function  $\chi(\omega)$  which is analytic in the closed upper half plane of  $\omega$  and vanishes like  $1/|\omega|$  or faster as  $|\omega| \rightarrow \infty$  and  $\chi(\omega) = \chi^*(-\omega)$ , we have

$$\text{Re} \chi(\omega) = \frac{2}{\pi} \int_0^\infty d\omega' \mathcal{P} \frac{\omega' \text{Im} \chi(\omega')}{\omega^2 - \omega'^2}. \quad (\text{B15})$$

Applying this to  $\omega^2 \mathbf{G}(\omega)$ , we obtain

$$F_{ij}(\omega) + F_{ij}(-\omega) = \frac{-\omega^2}{\hbar \epsilon_0 c^2} \mathbf{d}_i \cdot \text{Re} \mathbf{G}(\mathbf{r}_i, \mathbf{r}_j, \omega) \cdot \mathbf{d}_j, \quad (\text{B16})$$

which finally gives

$$\Lambda_{21} \rightarrow \frac{-\omega^2}{2\hbar \epsilon_0 c^2} \mathbf{d}_i \cdot \mathbf{G}(\mathbf{r}_i, \mathbf{r}_j, \omega) \cdot \mathbf{d}_j \equiv -h_{ij}, \quad (\text{B17a})$$

$$\Lambda_{12} \rightarrow \frac{-\omega^2}{2\hbar \epsilon_0 c^2} \mathbf{d}_i \cdot \mathbf{G}^*(\mathbf{r}_i, \mathbf{r}_j, \omega) \cdot \mathbf{d}_j = -h_{ij}^*. \quad (\text{B17b})$$

Together with  $\Lambda_{11} = 0$ , this yields the graphene-induced emitter-emitter coupling action  $S_{ee}^{(p)}$  given in Eq. (5). Note that the derivation of  $S_{ee}^{(p)}$  does not discard counterrotating-wave terms or apply the Markov approximation, which treats the  $\omega$  dependence of the spectrum as a constant.

### APPENDIX C: SPATIAL DISORDER

We define two matrices

$$V^1 = \sigma^x = \begin{pmatrix} 0 & 1 \\ 1 & 0 \end{pmatrix}, \quad V^2 = i \begin{pmatrix} 0 & -1 \\ 1 & 2 \text{sgn}(\omega) \end{pmatrix}. \quad (\text{C1})$$

Then  $S_{ee}^{(p)}$  can be put in the form

$$S_{ee}^{(p)} = \sum_{i,j=1}^N \int_{\omega} \text{Re} h_{ij}(\omega) v_{ij}^{(1)}(\omega) + \text{Im} h_{ij}(\omega) v_{ij}^{(2)}(\omega), \quad (\text{C2})$$

where

$$v_{ij}^{(a)}(\omega) = (\phi_{i,c} \quad \phi_{i,q})_{-\omega} \cdot V^a \cdot \begin{pmatrix} \phi_{j,c} \\ \phi_{j,q} \end{pmatrix}_{\omega}. \quad (\text{C3})$$

This form will facilitate the Gaussian averaging over the coupling strengths  $\text{Re} h_{ij}(\omega)$  and  $\text{Im} h_{ij}(\omega)$ . For terms with

subscript  $i \neq j$ , we assume a multicomponent Gaussian distribution (7a) and (7b). Different from the emitter-emitter coupling strength, the values of the graphene-induced individual terms  $\text{Re } h_{ii}(\omega)$  and  $\text{Im } h_{ii}(\omega)$  depend only on the distance from the emitter to the graphene. Since we have assumed that the layer of emitters is parallel to the graphene monolayer, all the  $h_{ii}(\omega)$  are fixed and identical. In Appendix F we present figures showing these coupling strengths and the elements of the covariance matrix.

To explore the phase transition at  $N \rightarrow \infty$ , we define

$$h_i^d = N \times h_{ii}, \quad h^o = N \times \bar{h}_{(2)}, \quad M^o = N \times M, \quad (\text{C4})$$

so after averaging over  $h_{ij}$  ( $i \neq j$ ) as described in the main text we have

$$\begin{aligned} \bar{S}_{ee}^{(p)} &= \frac{1}{N} \sum_{i=1}^N \int_{\omega} (h_i^d - h^o)_a(\omega) v_{ii}^{(a)}(\omega) \\ &+ \frac{1}{N} \sum_{i,j=1}^N \int_{\omega} h_a^o(\omega) v_{ij}^{(a)}(\omega) \\ &+ i \frac{1}{N} \sum_{i \neq j=1}^N \int_{\omega, \omega'} v_{ij}^{(a)}(\omega) M_{ab}^o(\omega, \omega') v_{ij}^{(b)}(\omega'), \quad (\text{C5}) \end{aligned}$$

where the summation over replicated indices  $a$  and  $b$  is implicitly assumed and we have written  $h^{d(o)}$  in the vector form of  $(\text{Re } h^{d(o)}, \text{Im } h^{d(o)})$ . While in the third line of Eq. (C5) terms with  $i = j$  are excluded, in the limit of large  $N$ , we may release this exclusion (see more discussion in Appendix E) and define

$$\begin{aligned} \Phi_{\alpha}(\omega) &= \sum_{i=1}^N \phi_{i,\alpha}(\omega), \\ \Phi_{\alpha\beta}(\omega, \omega') &= \sum_{i=1}^N \phi_{i,\alpha}(\omega) \phi_{i,\beta}(\omega'). \quad (\text{C6}) \end{aligned}$$

Now the Keldysh action can be expressed in terms of  $\Phi_{\alpha}$  and  $\Phi_{\alpha\beta}$ ,

$$\begin{aligned} S &= \frac{1}{N} \sum_{i=1}^N \int_{\omega} \phi_{i,\alpha}(-\omega) \phi_{i,\beta}(\omega) \Lambda_{i,\alpha\beta}^e(\omega) - 2 \sum_{i=1}^N \lambda_{i,q} 2\pi \delta(0) \\ &+ \frac{1}{N} \int_{\omega} \Phi_{\alpha}(-\omega) \Phi_{\beta}(\omega) \Lambda_{\alpha\beta}^{ce}(\omega) \\ &+ i \frac{1}{N} \int_{\omega, \omega'} \Phi_{\alpha\beta}(-\omega, -\omega') \tilde{M}_{\alpha\beta, \alpha'\beta'}(\omega, \omega') \Phi_{\alpha'\beta'}(\omega, \omega'), \quad (\text{C7}) \end{aligned}$$

where the new matrices are defined as

$$\begin{aligned} \Lambda_i^e &= N \begin{pmatrix} \lambda_{i,q} & \lambda_{i,c} - \frac{\omega^2}{\omega_i} \\ \lambda_{i,c} - \frac{\omega^2}{\omega_i} & \lambda_{i,q} \end{pmatrix} + (h_i^d - h^o)_a V^a, \\ \Lambda^{ce} &= h_a^o V^a, \\ \tilde{M}_{\alpha\beta, \alpha'\beta'}(\omega, \omega') &= \sum_{s,t} V_{\alpha\alpha'}^s(\omega) M_{st}^o(\omega, \omega') V_{\beta\beta'}^t(\omega'). \quad (\text{C8}) \end{aligned}$$

Then we apply the Hubbard-Stratonovich transformation based on the formula that

$$\begin{aligned} &\int D[\psi_{\alpha}] \exp \left( -iN \int_{\omega} \psi_{\alpha}(-\omega) \Lambda_{\alpha\beta}^{ce}(\omega) \psi_{\beta}(\omega) \right. \\ &\quad \left. - 2i \int_{\omega} \psi_{\alpha}(-\omega) \Lambda_{\alpha\beta}^{ce}(\omega) \phi_{\beta}(\omega) \right) \\ &\propto \exp \left( i \frac{1}{N} \int_{\omega} \phi_{\alpha}(-\omega) \Lambda_{\alpha\beta}^{ce}(\omega) \phi_{\beta}(\omega) \right). \quad (\text{C9}) \end{aligned}$$

The coefficient of proportionality in this formula is a constant, which is irrelevant to the dynamical variables. The Hubbard-Stratonovich transformation of  $\Phi_{\alpha\beta}$  is based on a similar formula of the Gaussian integral

$$\begin{aligned} &\int D[Q_a] \exp \left( -N \int_q Q_a(-q) \tilde{M}_{ab}(q) Q_b(q) \right. \\ &\quad \left. - 2i \int_q Q_{\alpha}(-q) \tilde{M}_{ab}(q) \Phi_b(q) \right) \\ &\propto \exp \left( -\frac{1}{N} \int_q \Phi_a(-q) \tilde{M}_{ab}(q) \Phi_b(q) \right), \quad (\text{C10}) \end{aligned}$$

where  $a$  and  $b$  denote the subscripts  $(\alpha\beta)$  and  $(\alpha'\beta')$ , and  $q$  is used to abbreviate  $(\omega, \omega')$ .

After the transformations, the Keldysh action has some residual  $\phi_i$  terms of order less than or equal to 2. We can eliminate these terms by Gaussian integrals.

Then the Keldysh action becomes a functional of the Lagrange multiplier  $\lambda_{i,\alpha}$  and the two new dynamical variables  $\psi_{\alpha}$  and  $Q_{\alpha\beta}$ , which are introduced in Eq. (9). Substituting the static ansatz at the mean-field level

$$\begin{aligned} \psi_{\alpha}(\omega) &= 2\pi \psi_{\alpha} \delta(0), \\ Q_{\alpha\beta}(\omega, \omega') &= Q_{\alpha\beta}(\omega) 2\pi \delta(\omega + \omega'), \quad (\text{C11}) \end{aligned}$$

this finally yields the action in terms of  $\psi_{\alpha}$ ,  $Q_{\alpha\beta}$ , and  $\lambda_i$ ,

$$\begin{aligned} S &= \frac{i}{2} \sum_{i=1}^N \text{tr} \ln(2\mathbf{L}_i) - 2 \sum_{i=1}^N \pi \delta(0) (\Lambda^{ce} \psi)^T \mathbf{L}_i^{-1}(0) (\Lambda^{ce} \psi) \\ &+ i 2\pi \delta(0) N \int_{\omega} Q_{\alpha\beta}(-\omega) \tilde{M}_{\alpha\beta, \alpha'\beta'}(\omega, -\omega) Q_{\alpha'\beta'}(\omega) \\ &- 2\pi \delta(0) N \psi_{\alpha} \Lambda_{\alpha\alpha'}^{ce}(0) \psi_{\alpha'} - 4\pi \delta(0) \sum_{i=1}^N \lambda_{i,q}, \quad (\text{C12}) \end{aligned}$$

where the matrix  $\mathbf{L}_i$  is defined as

$$\begin{aligned} \mathbf{L}_i(\omega, \omega') &= \mathbf{L}(\omega) 2\pi \delta(\omega + \omega'), \\ \mathbf{L}_{i,\alpha\beta}(\omega) &= \frac{1}{N} \Lambda_{i,\alpha\beta}^e(-\omega) \\ &\quad - 2Q_{\alpha'\beta'}(-\omega) \tilde{M}_{\alpha'\beta', \alpha\beta}(\omega, -\omega). \quad (\text{C13}) \end{aligned}$$

#### APPENDIX D: SADDLE-POINT EQUATIONS

We now turn to the solution of the saddle-point equations

$$\frac{\delta}{\delta q} S \stackrel{!}{=} 0, \quad q \in \{\lambda_{i,\alpha}, \psi_{\alpha}, Q_{\alpha\beta}\}, \quad (\text{D1})$$

which is restricted by the causality conditions  $\lambda_q = Q_{qq} = \psi_q = 0$ .

### 1. Equations for $\lambda_{i,\alpha}$

We assume  $\lambda_{i,\alpha} = \lambda_\alpha$  and replace the summation in Eq. (C12) with a factor of  $N$ . The saddle-point equation with respect to the Lagrangian multiplier  $\lambda_q$  is

$$\frac{i}{2} \int_\omega \text{tr}[\mathbf{L}_{\text{reg}}^{-1}(\omega)] - \frac{1}{\det \mathbf{L}(0)} [\psi_c^2 (\Lambda_{cq}^{ce})^2 + q_{\text{EA}} \tilde{M}_{cc,qq}(0)] - 2 = 0, \quad (\text{D2})$$

which confirms the restriction  $\phi_i^2 = 1$ . In Eq. (D2),  $\mathbf{L}_{\text{reg}}$  refers to the part defined with  $Q_{cc}^{\text{reg}}$ . The equation with respect to the Lagrangian multiplier  $\lambda_c$  is

$$-\frac{i}{2} \int_\omega \frac{1}{\det \mathbf{L}(\omega)} \text{tr}[\sigma_x \mathbf{L}(\omega)] = 0. \quad (\text{D3})$$

This equation is a statement of the universal property of the Keldysh Green's function that

$$Q^R(t, t) + Q^A(t, t) = 0, \quad (\text{D4})$$

where  $Q^R = Q_{cq}$  and  $Q^A = Q_{qc}$ .

### 2. Equations for $\psi_\alpha$

For  $\psi_c$ , the saddle-point equation is trivial because

$$(\Lambda^{ce})_{cc} = 0, \quad (\Lambda^{ce} \mathbf{L}^{-1} \Lambda^{ce})_{cc} = 0, \quad (\mathbf{L}^{-1})_{qq} = 0, \quad (\text{D5})$$

when  $\lambda_q = \psi_q = Q_{qq} = 0$ . For  $\psi_q$ , the saddle-point equation gives

$$\psi_c [\Lambda_{qc}^{ce} (\mathbf{L}^{-1})_{cq} + 1] = 0, \quad (\text{D6})$$

which gauges the relation between  $\lambda_c$  and  $Q_{cq}$ , in the SR phase where  $\psi_c \neq 0$ .

### 3. Equations for $Q_{\alpha\beta}^{\text{reg}}$

The Edwards-Anderson order parameter  $q_{\text{EA}}$  is introduced as the singular part of  $Q_{cc}(\omega)$ ,

$$Q_{cc}(\omega) = Q_{cc}^{\text{reg}}(\omega) - 2\pi i q_{\text{EA}} \delta(\omega), \quad (\text{D7})$$

and the saddle-point equation for the regular component reads

$$2Q_{\alpha\beta}^{\text{reg}}(\omega) = [\mathbf{L}(\omega)]_{\text{reg},\beta\alpha}^{-1} + 4i\pi \left( \frac{\psi_c^2 (\Lambda_{cq}^{ce})^2}{\det \mathbf{L}(0)} + q_{\text{EA}} + q_{\text{EA}} \frac{\tilde{M}_{cc,qq}(0)}{\det \mathbf{L}(0)} \right) \delta_{\alpha c} \delta_{\beta c} \delta(\omega). \quad (\text{D8})$$

Note that this equation can be separated into the regular part and the singular part at  $\omega = 0$ :

$$2Q_{\alpha\beta}^{\text{reg}} = [\mathbf{L}(\omega)]_{\text{reg},\beta\alpha}^{-1}, \quad (\text{D9a})$$

$$(\Lambda_{cq}^{ce})^2 \psi_c^2 = -q_{\text{EA}} [\tilde{M}_{cc,qq} + \det \mathbf{L}(0)]. \quad (\text{D9b})$$

For the regular part, implementing the substitution of Eq. (C13) for the  $cq$  component gives

$$\frac{1}{2Q_{cq}} = \lambda_c - \frac{\omega^2}{\omega_z} + \bar{h}_{(1)} - \bar{h}_{(2)} - 2Q_{cq} \tilde{M}_{qc,cq}(\omega, -\omega), \quad (\text{D10})$$

where we have assumed  $\lambda_{i,\alpha} = \lambda_\alpha$  for every emitter.

We find that this equation does not have a unique solution except in the absence of randomness,  $M \rightarrow 0$ , where the second line of Eq. (C12) vanishes and the Keldysh action attains the value given in Ref. [26]. We select the solution that is continuously connected to the unique solution to Eq. (D10) with  $\tilde{M} = 0$ , under the variation of  $\lambda \tilde{M}$ ,  $\lambda : 1 \rightarrow 0$ .

The regular part of  $Q_{cc}$  turns out to be

$$Q_{cc}^{\text{reg}} = \frac{4|Q_{cq}|^2}{1 - 4|Q_{cq}|^2 \tilde{M}_{cc,qq}(\omega, -\omega)} [Q_{qc} \tilde{M}_{cq,qq}(\omega, -\omega) + Q_{cq} \tilde{M}_{qc,cq}(\omega, -\omega) - i \text{sgn}(\omega) (\text{Im} \bar{h}_{(1)} - \text{Im} \bar{h}_{(2)})]. \quad (\text{D11})$$

The causality condition of the Keldysh formalism implies  $Q_{qq} = \lambda_{i,q} = \psi_q = 0$  and  $Q_{cq}(\omega) = Q_{qc}^*(\omega)$  [24].

Since the Edward-Anderson order parameter  $q_{\text{EA}}$  is non-negative, it follows from Eq. (D9b) that to have  $\psi_c^2 > 0$  we must have

$$\tilde{M}_{cc,qq}(0, 0) + \det \mathbf{L}(0) < 0. \quad (\text{D12})$$

This relation helps to distinguish the SR phase and the SG phase.

### 4. Determination of $\lambda_c$ and the three phases

In the SR phase,  $\psi_c \neq 0$ , so Eq. (D6) determines the value of  $\lambda_c^{\text{SR}}$ ,

$$\lambda_c^{\text{SR}} = -\bar{h}_{(1)}(0) + \bar{h}_{(2)}(0) - \Lambda_{qc} - \frac{N}{\Lambda_{qc}} M_{11}(0, 0), \quad (\text{D13})$$

where  $M_{11}$  is the real-real element of  $M$  and  $\Lambda_{qc} = N \text{Re} \bar{h}_{(2)}(0)$ . In the SG phase, we have  $q_{\text{EA}} > 0$  and  $\psi_c = 0$ . Therefore, the singular part of Eq. (D9) yields

$$\tilde{M}_{cc,qq}(0, 0) + \det \mathbf{L}(0) = 0. \quad (\text{D14})$$

Note that  $\det \mathbf{L}(0) = \frac{1}{4Q_{cq}Q_{qc}(0)}$ . Corresponding to the cases  $\frac{1}{2Q_{cq}(0)} = \pm \sqrt{\tilde{M}_{qc,cq}(0, 0)}$ , we have

$$\lambda_c^{\text{SG}} = -\frac{1}{N} [h^d(0) - h^o(0)] \pm 2\sqrt{N \times M_{11}(0)}. \quad (\text{D15})$$

The possibility of  $\lambda_c^{\text{SR}} = \lambda_c^{\text{SG}}$  corresponds to the minus sign of (D15). Thus we get

$$\lambda_c^{\text{SG}} = -\bar{h}_{(1)}(0) + \bar{h}_{(2)}(0) - 2\sqrt{N \times M_{11}(0, 0)}. \quad (\text{D16})$$



It turns out that the system is in the SR phase rather than the SG phase only if

$$[\bar{h}_{(2)}(0)]^2 > \frac{1}{N} M_{11}(0, 0). \quad (\text{D17})$$

This expression also gives the analytical result of the SG-SR phase boundary. In Appendix F we will elaborate on the calculation for the emitter-graphene system. We find that the values of  $\bar{h}_{(2)}(0)$  and  $M_{11}(0, 0)$  are insensitive to the graphene Fermi energy  $E_F$ .

For the normal phase,  $\lambda_c$  should be determined from the equality

$$\frac{i}{4\pi} \int_{-\infty}^{\infty} d\omega Q_{cc}^{\text{reg}}(\omega) = 2. \quad (\text{D18})$$

The boundaries between the normal phase and the other phases are obtained by matching their values of  $\lambda_c$ . The determination of  $q_{\text{EA}}$  and  $\psi_c$ , which are present in the singular part of  $Q_{cc}(\omega)$ , are obtained from the equality

$$\frac{i}{4\pi} \int_{-\infty}^{\infty} d\omega Q_{cc}(\omega) = 2. \quad (\text{D19})$$

#### APPENDIX E: INHOMOGENEOUS BROADENING

We suppose the emitters suffer from inhomogeneous broadening, so the transition frequency follows a Gaussian distribution

$$\rho(\omega_{i,z}) = \frac{1}{\sqrt{2\pi}\Delta} \exp\left(-\frac{(\omega_{i,z} - \omega_z)^2}{2\Delta^2}\right), \quad (\text{E1})$$

where  $\Delta$  is the standard deviation of  $\omega_{i,z}$ . The corresponding probability distribution of  $\frac{1}{\omega_{i,z}}$  is

$$\begin{aligned} p\left(\frac{1}{\omega_{i,z}}\right) &= \omega_{i,z}^2 \rho(\omega_{i,z}) \\ &= \frac{1}{\sqrt{2\pi}\Delta} \exp\left(2 \ln \omega_{i,z} - \frac{(\omega_{i,z} - \omega_z)^2}{2\Delta^2}\right). \end{aligned} \quad (\text{E2})$$

The condition  $\Delta \ll \omega_z$  implies that  $\ln \omega_{i,z} \approx \ln \omega_z + \omega_{i,z}/\omega_z - 1$ . Thus,  $1/\omega_{i,z}$  has a Gaussian distribution with variance  $\frac{\Delta}{\omega_z^2}$ ,

$$p\left(\frac{1}{\omega_{i,z}}\right) \approx \frac{\omega_z^2}{\sqrt{2\pi}\Delta} \exp\left(-\frac{(1/\omega_{i,z} - 1/\omega_z)^2}{2(\Delta/\omega_z^2)^2}\right). \quad (\text{E3})$$

We will average functions of  $\omega_{i,z}$  according to this distribution. Let us rewrite the Keldysh action of the free emitters (4), but replace  $\omega_z$  with  $\omega_{i,z}$ :

$$S_e = - \sum_{i=1}^N \sum_{a=\pm} a \int dt \frac{1}{\omega_{i,z}} (\partial_t \phi_{i,a})^2 + \lambda_{i,a}(t) (\phi_{i,a}^2 - 1). \quad (\text{E4})$$

Compared with the Keldysh action without inhomogeneous broadening, an additional term is obtained from the average of  $\omega_{i,z}$ , that is,

$$\begin{aligned} S^{(b)} &= i \frac{\Delta^2}{2\omega_z^4} \sum_{i=1}^N \int_{\omega, \omega'} \omega^2 \omega'^2 \phi_{i,c} \\ &\quad \times (-\omega) \phi_{i,q}(\omega) \phi_{i,c}(-\omega') \phi_{i,q}(\omega'). \end{aligned} \quad (\text{E5})$$

Note that the integrals over  $\omega$  and  $\omega'$  are independent and factor into a product. We recall that in Eq. (C5) we made

an approximation and released the restriction that  $i \neq j$ . We can reintroduce the restriction by incorporating the individual terms with  $i = j$  and obtain the action

$$S^{(b)} - i \frac{1}{N} \sum_{i=1}^N \int_{\omega, \omega'} v_{ii}^{(a)}(\omega) M_{ab}^o(\omega, \omega') v_{ii}^{(b)}(\omega'). \quad (\text{E6})$$

To cope with the fourth-order terms, we will apply the Hubbard-Stratonovich transformation.

Let us define  $\Phi_{\alpha\beta}^i(\omega, \omega') = \phi_{i,\alpha}(\omega) \phi_{i,\beta}(\omega')$ . Then Eq. (E6) can be rewritten as

$$i \sum_{i=1}^N \int_{\omega, \omega'} \Phi_{\alpha\beta}^i(-\omega, -\omega') \delta \tilde{M}_{\alpha\beta, \alpha'\beta'}(\omega, \omega') \Phi_{\alpha'\beta'}^i(\omega, \omega'), \quad (\text{E7})$$

where the matrix  $\delta \tilde{M}_{\alpha\beta, \alpha'\beta'}(\omega, \omega')$  is defined as

$$\begin{aligned} \delta \tilde{M}_{\alpha\beta, \alpha'\beta'}(\omega, \omega') &= -\frac{1}{N} \tilde{M}_{\alpha\beta, \alpha'\beta'}(\omega, \omega') + \omega^2 \omega'^2 \frac{\Delta^2}{8\omega_z^4} (\delta_{\alpha\beta, cq} \delta_{\alpha'\beta', qc} \\ &\quad + \delta_{\alpha\beta, qc} \delta_{\alpha'\beta', cq} + \delta_{\alpha\beta, cc} \delta_{\alpha'\beta', qq} + \delta_{\alpha\beta, qq} \delta_{\alpha'\beta', cc}). \end{aligned} \quad (\text{E8})$$

We can implement the Hubbard-Stratonovich transformation of Eq. (E7) in a way similar to Eq. (C10),

$$\begin{aligned} &\int D[Q_a^i] \exp\left(-N \int_q Q_a^i(-q) \tilde{M}_{ab}(q) Q_b^i(q) \right. \\ &\quad \left. - 2i \int_q Q_\alpha^i(-q) \tilde{M}_{ab}(q) \Phi_b(q)\right) \\ &\propto \exp\left(-\frac{1}{N} \int_q \Phi_a^i(-q) \tilde{M}_{ab}(q) \Phi_b^i(q)\right), \end{aligned} \quad (\text{E9})$$

where the conventions of notation are the same as in Eq. (C10). In the sense of saddle-point equations, the physical meaning of  $Q_{\alpha\beta}^i$  is

$$Q_{\alpha\beta}^i = \langle \phi_{i,\alpha} \phi_{i,\beta} \rangle. \quad (\text{E10})$$

By the further assumption of the homogeneous mean-field ansatz that for all  $i$ ,

$$\langle \phi_{i,\alpha} \phi_{i,\beta} \rangle = \frac{1}{N} \sum_{k=1}^N \langle \phi_{k,\alpha} \phi_{k,\beta} \rangle, \quad (\text{E11})$$

we can replace the new variable  $Q_{\alpha\beta}^i$  with  $Q_{\alpha\beta}$ , which is defined in the context of spatial disorders.

The result of all the above steps can also be obtained by rewriting Eq. (E6) as

$$i \frac{1}{N} \int_{\omega, \omega'} \Phi_{\alpha\beta}(-\omega, -\omega') \delta \tilde{M}_{\alpha\beta, \alpha'\beta'}(\omega, \omega') \Phi_{\alpha'\beta'}(\omega, \omega') \quad (\text{E12})$$

followed by the Hubbard-Stratonovich transformation in a way similar to Eq. (C10). It means that the effect of inhomogeneous broadening can be seen as a modification of the matrix  $\tilde{M}$  defined in Eq. (C7) by a term  $\delta \tilde{M}$  given in Eq. (E8).

Note that the first term of Eq. (E7) comes from the additional term mentioned in Eq. (E6) and contributes only little when  $N \gg 1$ , thus justifying the approximation made for Eq. (C7). Since  $\tilde{M}$  is defined with a factor of  $N$  [see Eq. (C4)],

the correction made by inhomogeneous broadening [Eq. (E8)] is also negligible when  $N$  is large.

### APPENDIX F: THE SPECIFIC EXAMPLE OF THE EMITTER-GRAPHENE SYSTEM

The surface conductivity of the graphene monolayer is

$$\sigma(E_F, \tau; \omega) = \frac{e^2 E_F}{\pi \hbar^2} \frac{i}{\omega + i\tau^{-1}} + \frac{e^2}{4\hbar} \left( \Theta(\hbar\omega - 2E_F) + \frac{i}{\pi} \ln \left| \frac{\hbar\omega - 2E_F}{\hbar\omega + 2E_F} \right| \right). \quad (\text{F1})$$

When the emitter dipoles are aligned perpendicular to the graphene monolayer, the relevant element of the dyadic Green's tensor is  $\mathbf{G}_{zz}^0 + \mathbf{G}_{zz}^s$ , where  $\mathbf{G}_{zz}^0$  is the vacuum dyadic Green's function for free propagation modes and  $\mathbf{G}_{zz}^s$  is the so-called scattering part accounting for the surface plasmon modes of the graphene monolayer

$$\begin{aligned} \frac{\omega^2}{c^2} \mathbf{G}_{zz}^s(\mathbf{r}, \mathbf{r}'; z) &= \int \frac{d^2 \mathbf{k}_{\parallel}}{(2\pi)^2} \frac{i}{2\epsilon_1 k_{1,z}} k_{\parallel}^2 r_p e^{i\mathbf{k}_{\parallel} \cdot \delta \mathbf{r} + 2i k_{1,z} z} \\ &= \int \frac{dk_{\parallel}}{2\pi} \frac{i}{2\epsilon_1 k_{1,z}} k_{\parallel}^3 r_p J_0(k_{\parallel} \delta r), e^{2i k_{1,z} z}, \end{aligned} \quad (\text{F2})$$

where  $\delta \mathbf{r} = \mathbf{r} - \mathbf{r}'$  and  $\delta r$  is its length;  $J_0$  is the zeroth-order Bessel function;  $\epsilon_{1(2)}$  is the relative permittivity of the dielectric above (below) the graphene monolayer, and  $r_p$  is the Fresnel coefficient of reflection of the  $p$  modes from above the graphene layer

$$r_p = \frac{-\epsilon_1 k_{2,z} + \epsilon_2 k_{1,z} + \frac{\sigma(\omega)}{\omega \epsilon_0} k_{1,z} k_{2,z}}{\epsilon_1 k_{2,z} + \epsilon_2 k_{1,z} + \frac{\sigma(\omega)}{\omega \epsilon_0} k_{1,z} k_{2,z}}, \quad (\text{F3})$$

where  $k_{1(2),z} = \sqrt{\frac{\omega^2}{c^2} \epsilon_{1(2)} - k_{\parallel}^2}$ . Note that in the limit  $\omega \rightarrow 0$ ,  $r_p$  equals 1 and does not depend on the Fermi energy. As a result, the Fermi energy  $E_F$  is irrelevant to the SG-SR boundary.

In the numerical calculation, it is convenient to normalize  $k_{\parallel}$  and  $\delta r$  in the above expressions by  $\omega_z/c$ . That is, define

$$k_{\parallel} = \frac{\omega}{c} \tilde{k}_{\parallel}, \quad \delta r = \frac{c}{\omega_z} \delta \tilde{r}, \quad z = \frac{c}{\omega_z} \tilde{z} \quad (\text{F4})$$

and then Eq. (F2) is recast as

$$\left( \frac{\omega_z}{c} \right)^3 \int_0^{\infty} \frac{d\tilde{k}_{\parallel}}{2\pi} \frac{i}{2\epsilon_1 \tilde{k}_{1,z}} \tilde{k}_{\parallel}^3 r_p J_0(\tilde{k}_{\parallel} \delta \tilde{r}) e^{2i \tilde{k}_{1,z} \tilde{z}}. \quad (\text{F5})$$

The factor  $(\frac{\omega_z}{c})^3$  can then be combined with the length of  $\mathbf{d}_i$  and absorbed into the expression for the vacuum spontaneous-emission rate  $\gamma_0$ . The surface-plasmons have the dispersion relation

$$\epsilon_1 k_{2,z}^{sp} + \epsilon_2 k_{1,z}^{sp} + \frac{\sigma(\omega_{sp})}{\omega_{sp} \epsilon_0} k_{1,z}^{sp} k_{2,z}^{sp} = 0, \quad (\text{F6})$$

where  $k_{1(2),z} = \sqrt{\frac{\omega^2}{c^2} \epsilon_{1(2)} - k_{sp}^2}$ , and  $\omega_{sp}$  and  $k_{sp}$  represent the frequency and wave vector of the surface-plasmon, respectively.

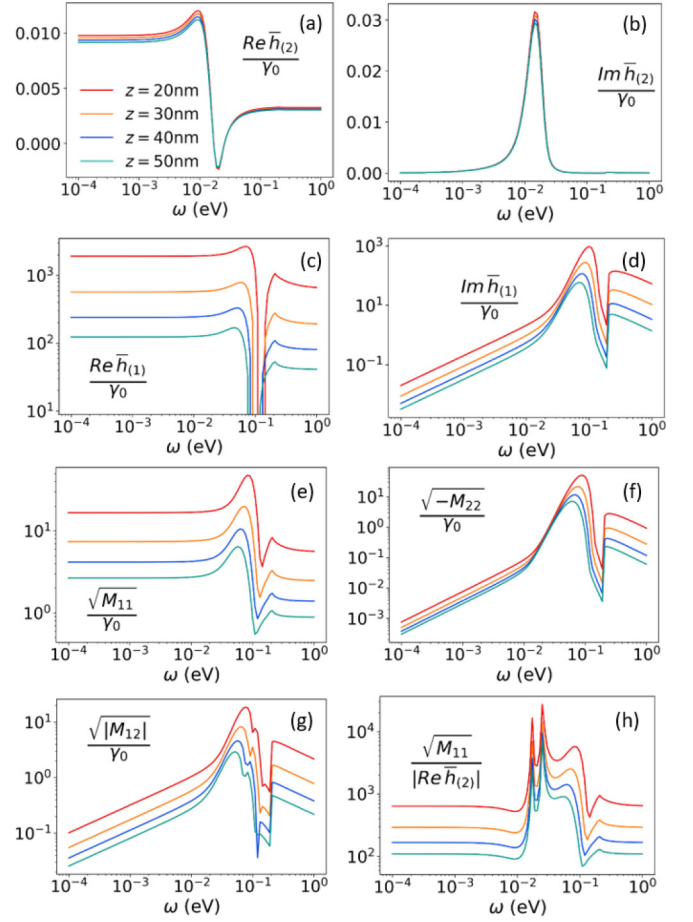


FIG. 4. Coefficients of the emitter-graphene-surface-plasmon coupling for systems with  $\omega_z = 0.5$  eV,  $E_F = 0.1$  eV, and  $L = 10^3$  nm. From the top to the bottom in the figures we show results for the different heights  $z = 20$  (red top curve),  $z = 30$  (orange curve),  $z = 40$  (blue curve), and  $z = 50$  (green bottom curve) nm. The dimensionless values are normalized by the emitter spontaneous-emission rate  $\gamma_0$ .

The horizontal coordinates  $\{(x_i, y_i)\}_i$  of the emitters are assumed to follow the identical Gaussian distribution

$$p(x, y) = \frac{1}{2\pi L^2} \exp\left(-\frac{x^2 + y^2}{2L^2}\right) \quad (\text{F7})$$

and the distance between any two emitters follows the distribution

$$p_L(\delta r) = \frac{\delta r}{2L^2} \exp\left(-\frac{(\delta r)^2}{4L^2}\right). \quad (\text{F8})$$

To calculate the mean values and covariances  $\bar{h}_{(1)}(\omega)$ ,  $\bar{h}_{(2)}(\omega)$ , and  $\tilde{M}(\omega, \omega')$  required in our formalism, the use of the Gaussian distribution permits analytical handling of the oscillating integrands related to the Bessel function  $J_0(k\delta r)$ ,

$$\begin{aligned} \int_0^{\infty} dr \frac{r}{2L^2} J_0(kr) \exp\left(-\frac{r^2}{4L^2}\right) &= \exp(-k^2 L^2), \\ \int_0^{\infty} dr \frac{r}{2L^2} J_0(kr) J_0(k'r) \exp\left(-\frac{r^2}{4L^2}\right) &= I_0(2L^2 k k') \exp[-L^2(k^2 + k'^2)], \end{aligned} \quad (\text{F9})$$

where  $I_0$  is the modified Bessel function. By use of these formulas, the remaining integrals are numerically well behaved.

Finally, to have an impression of the numerical results, we illustrate the  $z$  dependence of the averaged coupling strength and the elements of the covariance matrix in Fig. 4. It shows

that by decreasing  $z$ , the graphene SP-induced self-interaction terms and the elements of the covariance matrix are increased significantly, while the SP-induced emitter-emitter coupling strength changes little. This confirms our argument about the  $z$  dependence made in the main text.

- 
- [1] R. H. Dicke, *Phys. Rev.* **93**, 99 (1954).  
 [2] K. Hepp and E. H. Lieb, *Ann. Phys. (NY)* **76**, 360 (1973).  
 [3] Y. K. Wang and F. T. Hioe, *Phys. Rev. A* **7**, 831 (1973).  
 [4] V. Emeljanov and Y. Klimontovich, *Phys. Lett. A* **59**, 366 (1976).  
 [5] K. Gawędzki and K. Rzażewski, *Phys. Rev. A* **23**, 2134 (1981).  
 [6] M. Bamba and T. Ogawa, *Phys. Rev. A* **90**, 063825 (2014).  
 [7] J. Keeling, *J. Phys.: Condens. Matter* **19**, 295213 (2007).  
 [8] A. Vukics and P. Domokos, *Phys. Rev. A* **86**, 053807 (2012).  
 [9] A. Vukics, T. Griebner, and P. Domokos, *Phys. Rev. Lett.* **112**, 073601 (2014).  
 [10] A. Vukics, T. Griebner, and P. Domokos, *Phys. Rev. A* **92**, 043835 (2015).  
 [11] T. Griebner, A. Vukics, and P. Domokos, *Phys. Rev. A* **94**, 033815 (2016).  
 [12] T. Jaako, Z.-L. Xiang, J. J. Garcia-Ripoll, and P. Rabl, *Phys. Rev. A* **94**, 033850 (2016).  
 [13] D. De Bernardis, T. Jaako, and P. Rabl, *Phys. Rev. A* **97**, 043820 (2018).  
 [14] K. Baumann, C. Guerlin, F. Brennecke, and T. Esslinger, *Nature (London)* **464**, 1301 (2010).  
 [15] K. Baumann, R. Mottl, F. Brennecke, and T. Esslinger, *Phys. Rev. Lett.* **107**, 140402 (2011).  
 [16] F. Brennecke, R. Mottl, K. Baumann, R. Landig, T. Donner, and T. Esslinger, *Proc. Natl. Acad. Sci. USA* **110**, 11763 (2013).  
 [17] M. P. Baden, K. J. Arnold, A. L. Grimsmo, S. Parkins, and M. D. Barrett, *Phys. Rev. Lett.* **113**, 020408 (2014).  
 [18] J. Klinder, H. Keßler, M. Wolke, L. Mathey, and A. Hemmerich, *Proc. Natl. Acad. Sci. USA* **112**, 3290 (2015).  
 [19] Z. Zhiqiang, C. H. Lee, R. Kumar, K. J. Arnold, S. J. Masson, A. S. Parkins, and M. D. Barrett, *Optica* **4**, 424 (2017).  
 [20] F. Dimer, B. Estienne, A. S. Parkins, and H. J. Carmichael, *Phys. Rev. A* **75**, 013804 (2007).  
 [21] D. Tolkunov and D. Solenov, *Phys. Rev. B* **75**, 024402 (2007).  
 [22] S. Gopalakrishnan, B. L. Lev, and P. M. Goldbart, *Phys. Rev. Lett.* **107**, 277201 (2011).  
 [23] P. Strack and S. Sachdev, *Phys. Rev. Lett.* **107**, 277202 (2011).  
 [24] L. M. Sieberer, M. Buchhold, and S. Diehl, *Rep. Prog. Phys.* **79**, 096001 (2016).  
 [25] M. Buchhold, P. Strack, S. Sachdev, and S. Diehl, *Phys. Rev. A* **87**, 063622 (2013).  
 [26] E. G. D. Torre, S. Diehl, M. D. Lukin, S. Sachdev, and P. Strack, *Phys. Rev. A* **87**, 023831 (2013).  
 [27] P. Kirton and J. Keeling, *Phys. Rev. Lett.* **118**, 123602 (2017).  
 [28] V. M. Bastidas, C. Emary, B. Regler, and T. Brandes, *Phys. Rev. Lett.* **108**, 043003 (2012).  
 [29] O. Viehmann, J. von Delft, and F. Marquardt, *Phys. Rev. Lett.* **107**, 113602 (2011).  
 [30] M. Bamba, K. Inomata, and Y. Nakamura, *Phys. Rev. Lett.* **117**, 173601 (2016).  
 [31] L. J. Zou, D. Marcos, S. Diehl, S. Putz, J. Schmiedmayer, J. Majer, and P. Rabl, *Phys. Rev. Lett.* **113**, 023603 (2014).  
 [32] N. Lambert, C. Emary, and T. Brandes, *Phys. Rev. Lett.* **92**, 073602 (2004).  
 [33] C. Emary and T. Brandes, *Phys. Rev. Lett.* **90**, 044101 (2003).  
 [34] M. S. Tame, K. R. McEnery, K. Özdemir, J. Lee, S. A. Maier, and M. S. Kim, *Nat. Phys.* **9**, 329 (2013).  
 [35] P. Törmä and W. L. Barnes, *Rep. Prog. Phys.* **78**, 013901 (2015).  
 [36] D. E. Chang, A. S. Sørensen, P. R. Hemmer, and M. D. Lukin, *Phys. Rev. Lett.* **97**, 053002 (2006).  
 [37] W. Zhang, A. O. Govorov, and G. W. Bryant, *Phys. Rev. Lett.* **97**, 146804 (2006).  
 [38] V. N. Pustovit and T. V. Shahbazyan, *Phys. Rev. Lett.* **102**, 077401 (2009).  
 [39] V. N. Pustovit and T. V. Shahbazyan, *Phys. Rev. B* **82**, 075429 (2010).  
 [40] D. N. Basov, M. M. Fogler, and F. J. García de Abajo, *Science* **354**, aag1992 (2016).  
 [41] A. N. Grigorenko, M. Polini, and K. S. Novoselov, *Nat. Photon.* **6**, 749 (2012).  
 [42] F. H. L. Koppens, D. E. Chang, and F. J. García de Abajo, *Nano Lett.* **11**, 3370 (2011).  
 [43] K. J. Tielrooij, L. Orona, A. Ferrier, M. Badioli, G. Navickaite, S. Coop, S. Nanot, B. Kalinic, T. Cesca, L. Gaudreau, Q. Ma, A. Centeno, A. Pesquera, A. Zurutuza, H. de Riedmatten, P. Goldner, F. J. García de Abajo, P. Jarillo-Herrero, and F. H. L. Koppens, *Nat. Phys.* **11**, 281 (2015).  
 [44] A. J. Leggett, S. Chakravarty, A. T. Dorsey, M. P. A. Fisher, A. Garg, and W. Zwerger, *Rev. Mod. Phys.* **59**, 1 (1987).  
 [45] P. P. Orth, D. Roosen, W. Hofstetter, and K. Le Hur, *Phys. Rev. B* **82**, 144423 (2010).  
 [46] A. Winter and H. Rieger, *Phys. Rev. B* **90**, 224401 (2014).  
 [47] B. Huttner and S. M. Barnett, *Phys. Rev. A* **46**, 4306 (1992).  
 [48] A. Drezet, *Phys. Rev. A* **95**, 023831 (2017).  
 [49] T. G. Philbin, *New J. Phys.* **12**, 123008 (2010).  
 [50] T. Gruner and D.-G. Welsch, *Phys. Rev. A* **53**, 1818 (1996).  
 [51] H. T. Dung, L. Knöll, and D.-G. Welsch, *Phys. Rev. A* **57**, 3931 (1998).  
 [52] S. F. Edwards and P. W. Anderson, *J. Phys. F* **5**, 965 (1975).  
 [53] D. Dzsotjan, A. S. Sørensen, and M. Fleischhauer, *Phys. Rev. B* **82**, 075427 (2010).  
 [54] J. B. Kogut, *Rev. Mod. Phys.* **51**, 659 (1979).  
 [55] J. Ye, S. Sachdev, and N. Read, *Phys. Rev. Lett.* **70**, 4011 (1993).  
 [56] M. P. Kennett, C. Chamon, and J. Ye, *Phys. Rev. B* **64**, 224408 (2001).  
 [57] S. Sachdev, *Quantum Phase Transitions*, 2nd ed. (Cambridge University Press, Cambridge, 2011), Chap. 5.5.3.  
 [58] H. Aoki, N. Tsuji, M. Eckstein, M. Kollar, T. Oka, and P. Werner, *Rev. Mod. Phys.* **86**, 779 (2014).  
 [59] K. H. Fischer and J. A. Hertz, *Spin Glasses*, Cambridge Studies in Magnetism Book 1 (Cambridge University Press, Cambridge, 1993).  
 [60] H. Goto and K. Ichimura, *Phys. Rev. A* **77**, 053811 (2008).

- [61] G. W. Hanson, *J. Appl. Phys.* **103**, 064302 (2008).
- [62] A. Principi, G. Vignale, M. Carrega, and M. Polini, *Phys. Rev. B* **88**, 195405 (2013).
- [63] A. Woessner, M. B. Lundeberg, Y. Gao, A. Principi, P. Alonso-González, M. Carrega, K. Watanabe, T. Taniguchi, G. Vignale, M. Polini, J. Hone, R. Hillenbrand, and F. H. L. Koppens, *Nat. Mater.* **14**, 421 (2014).
- [64] Q.-J. Tong, J.-H. An, H.-G. Luo, and C. H. Oh, *Phys. Rev. A* **81**, 052330 (2010).
- [65] C.-J. Yang and J.-H. An, *Phys. Rev. B* **95**, 161408 (2017).
- [66] I. Thanopoulos, V. Yannopoulos, and E. Paspalakis, *Phys. Rev. B* **95**, 075412 (2017).
- [67] A. González-Tudela, P. A. Huidobro, L. Martín-Moreno, C. Tejedor, and F. J. García-Vidal, *Phys. Rev. B* **89**, 041402 (2014).
- [68] A. González-Tudela, F. J. Rodríguez, L. Quiroga, and C. Tejedor, *Phys. Rev. B* **82**, 115334 (2010).
- [69] S. Ashhab and K. Semba, *Phys. Rev. A* **95**, 053833 (2017).
- [70] H. T. Dung, L. Knöll, and D.-G. Welsch, *Phys. Rev. A* **66**, 063810 (2002).
- [71] I. de Vega and D. Alonso, *Rev. Mod. Phys.* **89**, 015001 (2017).
- [72] P. Rotondo, E. Tesio, and S. Caracciolo, *Phys. Rev. B* **91**, 014415 (2015).
- [73] P. Rotondo, M. Cosentino Lagomarsino, and G. Viola, *Phys. Rev. Lett.* **114**, 143601 (2015).
- [74] J. T. Stewart, J. P. Gaebler, and D. S. Jin, *Nature (London)* **454**, 744 (2008).
- [75] R. Haussmann, M. Punk, and W. Zwerger, *Phys. Rev. A* **80**, 063612 (2009).
- [76] Y. Kudenko, A. Slivinsky, and G. Zaslavsky, *Phys. Lett. A* **50**, 411 (1975).
- [77] J. H. Wesenberg and K. Mølmer, *Phys. Rev. Lett.* **93**, 143903 (2004).